

Ya.M. Chornodolskyi¹, V.O. Karnaushenko¹, S.O. Ihnatsevych¹, A.S. Voloshinovskii¹,
S.V. Syrotyuk², P.I. Vankevych³, P.A. Bolkot³, A.Y. Derevjanchuk⁴

Energy structure of mixed halide CeF₂Cl and CeFCl₂ crystals

¹Ivan Franko National University of Lviv, Lviv, Ukraine, yaroslav.chornodolskyi@lnu.edu.ua

²Lviv Polytechnic National University, Lviv, Ukraine

³Hetman Petro Sahaidachnyi National Army Academy, Lviv, Ukraine

⁴Sumy State University, Sumy, Ukraine

The band energy structures of CeF₂Cl and CeFCl₂ crystals have been calculated using the projector augmented-wave (PAW) method and the hybrid exchange-correlation functional PBE0. The valence band top consists of 2p states of F and 3p states of Cl. An energy gap is observed between the 5d states of Ce in the bottom part of the conduction band of both crystals, forming two subbands, 5d1 and 5d2, with very different effective electron masses (2.49 m₀ and 0.19 m₀ for CeF₂Cl and 5.95 m₀ and 0.84 m₀ for CeFCl₂, respectively). The 4f states of Ce are placed within the forbidden band. The obtained values for the band gap of CeF₂Cl and CeFCl₂ crystals are 6 eV and 4.6 eV, respectively.

Keywords: scintillator, band structure, density of states, exciton, projector augmented-wave method.

Received 04 February 2024; Accepted 03 May 2024.

Introduction

Inorganic crystals of lanthanide fluorides have proven themselves as excellent scintillators with applications spanning various fields of science and technology, including medicine, high-energy physics, radiation security, and space technologies [1]. The luminescent characteristics of these crystals are determined by their energy structure, particularly the positioning of lanthanide 4f and 5d states relative to the top of the valence band and the bottom part of the conduction band, and their band gap.

Previous studies [2-5] have analyzed the series of CeX₃ crystals (X = F, Cl, Br, I), but research on the further improvement of scintillation properties of lanthanide halide crystals is still relevant. A promising direction for investigations lies in exploring the crystal structures with mixed halogens, as it introduces new possibilities for controlling the band gap, directly influencing the light output in such scintillators [6]. Additionally, this approach improves the temperature stability of crystal luminescence and their radiation resistance by utilizing halogens with a higher atomic number.

Theoretical investigations on the energy structure of

crystals belonging to the CeCl_{3-x}Br_x and CeBr_{3-x}I_x families have been previously reported in works [7, 8]. This study represents the completion of this research cycle, providing data for CeF_{3-x}Cl_x crystals.

It is anticipated that CeF₂Cl and CeFCl₂ crystals will exhibit luminescent properties like CeF₃ and CeCl₃ crystals. Thus, it is crucial to highlight the fundamental scintillation characteristics of these materials. The fluorescence spectrum of CeF₃ is recognized for its characteristic doublet with peaks at 290 nm and 340 nm [9]. The former is caused by the 5d→4f transition in the Ce³⁺ ion [10] with fast decay kinetics [11]. CeF₃ crystal demonstrates a relatively high light output of 2400 photons/MeV [12].

In contrast, the CeCl₃ crystal has a significantly higher fluorescence light output corresponding to CeF₃, amounting to 46000 photons/MeV [13]. Additionally, this crystal has a substantially lower temperature dependence of luminescence compared to a structurally similar LaCl₃:Ce (5%) crystal, as it lacks transitions from the 5d states of cerium to the bottom part of the conduction band, which negatively impacts the temperature stability of the LaCl₃:Ce decay constant [14]. The major peaks in the

CeCl₃ crystal's fluorescence spectrum, caused by irradiation with energies of 4 eV and 5.4 eV, are analogous to LaCl₃:Ce and characterized by positions at 3.7 eV and 3.4 eV, respectively [14].

I. Calculations

All calculations have been conducted within the density functional theory (DFT) framework utilizing the projector augmented-wave (PAW) method. Nevertheless, in its conventional form, this approach has two notable deficiencies. There is an underestimation of the band gap [15], which complicates the interpretation of acquired data, given that CeF₃ crystal belongs to the class of wide-bandgap dielectrics [16]. Additionally, famous exchange-correlation functionals, such as the local density approximation (LDA) [17] or its gradient-corrected improvement, generalized gradient approximation (GGA) [18], are constructed based on the model of a homogeneous electron gas, which can be a too strong approximation in the presence of strongly localized states of lanthanide 4f and 5d electrons. Therefore, to investigate the electronic structure of CeF₂Cl and CeFCl₂ crystals, the hybrid exchange-correlation functional PBE0 has been used, which was efficient in similar theoretical studies [7, 8]. In these calculations, the parameter α was set to 0.25.

Before starting calculations, computer models of the investigated crystal cells have been constructed. For their assembly, lattice parameters of CeF₃ [19] and CeCl₃ [20] crystals have been taken from the Materials Project open database. Each lattice contains eight ions in the elementary cell (two cerium ions and six ions of the respective halogen). To create models of CeF₂Cl crystals within the CeF₃ crystal structure, two fluorine ions were replaced by two chlorine ions. A similar procedure has been performed to model CeFCl₂ but using the CeCl₃ lattice instead. In both cases, after completing the construction of the computer lattice models, a BFGS geometric optimization procedure has been done [21].

In the calculations the following parameters have been used: the size of Monkhorst-Pack is 10x10x10; energy cutoff for constructing the plane wave basis – 48 Hartree (1306 eV) beyond the PAW sphere and 108 Hartree (2938 eV) within the augmentation sphere; number of bands - 200.

All calculations were performed using the open-

source software ABINIT [22], which incorporates all the aforementioned theoretical approaches.

II. Results and Discussions

Figure 1 depicts the calculated partial densities of states for CeF₂Cl and CeFCl₂ crystals. The peaks in the valence bands of both crystals originate from the hybridized p-states of halogens, specifically 2p F and 3p Cl. The 4f levels of the cerium ion are placed within the forbidden band. The energy gap between the top of the valence band and 4f states band is 3.7 eV for CeF₂Cl and 2.6 eV for CeFCl₂. The bottom part of the conduction band is formed by the 5d levels of cerium.

From the density of states plots (Figure 2), it is evident that the valence bandwidth is 2.3 eV for CeF₂Cl and 2.9 eV for CeFCl₂. For both crystals, a significant intensity variation in the density of states of the conduction band (in the proximity of 8 eV for CeF₂Cl and 7 eV for CeFCl₂) can be observed. The obtained information about the energy structure of the studied crystals suggests the existence of two energetically separated subbands, 5d1 and 5d2, akin to what has been demonstrated for other crystals of the serial [7, 8, 23].

Figure 3 illustrates the band energy structure of the investigated crystals. The difference in the dispersion of the states at the bottom of the conduction bands can be distinguished visually (marked by square brackets beside the right axes of the diagrams). To confirm the presence of subbands 5d1 and 5d2 in the conduction band of the studied crystals, effective masses of electrons in these subbands were calculated in the proximity of the Γ point (where the band gap in both cases has its minimum). The calculated values are $m^* = 2.49 m_0$ for the 5d1 subband and $m^* = 0.19 m_0$ for the 5d2 subband of CeF₂Cl and $m^* = 5.95 m_0$ for the 5d1 subband and $m^* = 0.84 m_0$ for the 5d2 subband of CeFCl₂. Such values confirm the existence of a subband of localized states in the lower part of the conduction band, suggesting the potential for promising luminescent properties due to the effective formation of self-localized Frenkel excitons resulting from the 4f \rightarrow 5d1 transitions. The calculated band gaps are 6 eV and 4.6 eV for CeF₂Cl and CeFCl₂, respectively.

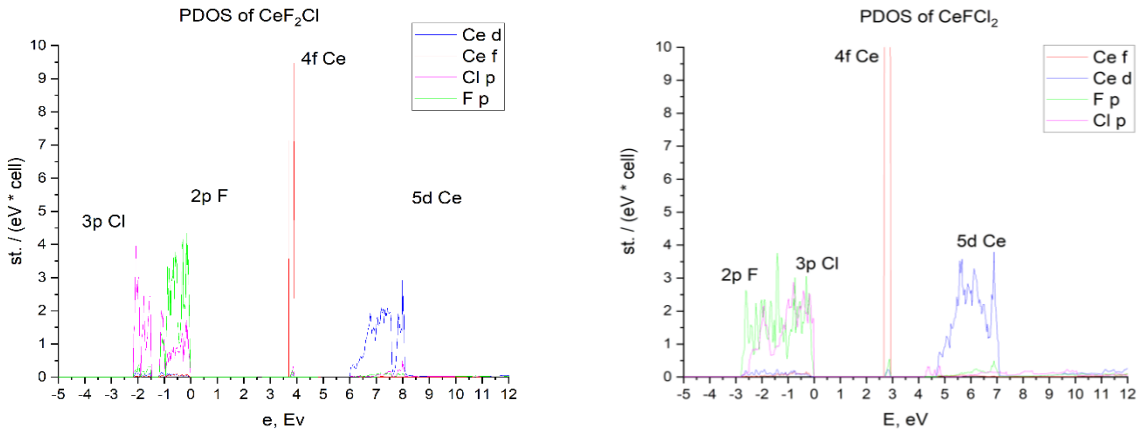


Fig. 1. Partial density of states of CeF₂Cl and CeFCl₂ crystals.

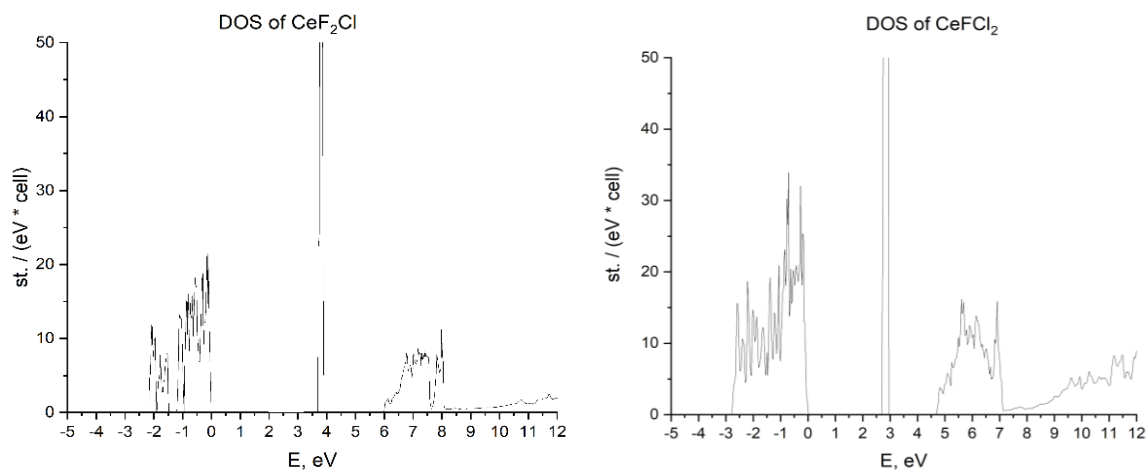


Fig. 2. Density of states of CeF_2Cl and CeFCl_2 crystals.

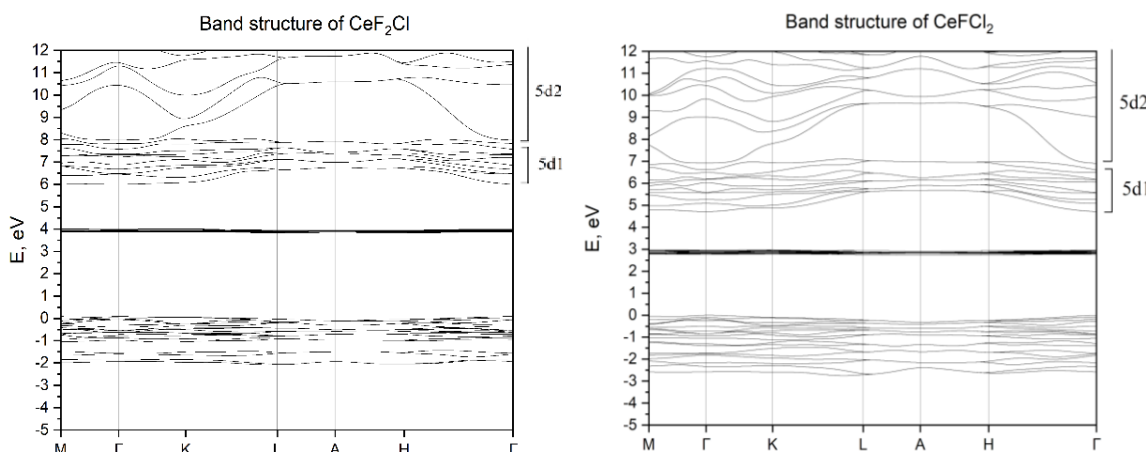


Fig. 3. Energy band structure CeF_2Cl and CeFCl_2 crystals.

Figure 4 presents the energy level diagram of $\text{CeF}_{3-x}\text{Cl}_x$ crystals. To construct this diagram, we used data from the current study and previous investigations of CeCl_3 [23] and CeF_3 [24] crystals. The diagram highlights a certain similarity in the energy structures of CeF_3 and CeF_2Cl , as well as CeFCl_2 and CeCl_3 crystals. It is crucial to note that, unlike the series of $\text{CeCl}_{3-x}\text{Br}_x$ and $\text{CeBr}_{3-x}\text{I}_x$ crystals, whose synthesis was successfully carried out in [25] and [26], the investigation of the $\text{CeF}_{3-x}\text{Cl}_x$ series remains purely theoretical.

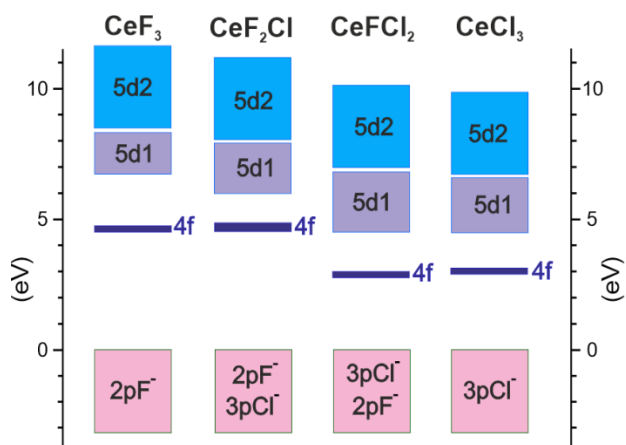


Fig. 4. Calculated energy band schema of CeF_3 , CeF_2Cl , CeFCl_2 and CeCl_3 crystals.

Conclusions

Using the projector augmented-wave (PAW) method and the hybrid exchange-correlation functional PBE0, we computed the partial and total density of states, as well as the band energy structure of cerium crystals with mixed halides CeF_2Cl and CeFCl_2 .

It was determined that the valence band of the crystals is formed through the hybridization of halogen p-states (2p F and 3p Cl). The 4f states of cerium are located within the forbidden band gap. The bottom part of the conduction band is composed of Ce 5d states. The calculated band gap widths are 6 eV and 4.6 eV for CeF_2Cl and CeFCl_2 , respectively.

It has been demonstrated that both crystals have a peculiarity in the form of energetically separated subbands 5d1 and 5d2 in the lower part of the conduction band, characterized by different effective masses of electrons in these states (CeF_2Cl : $m^* = 2.49 m_0$ and $m^* = 0.19 m_0$; CeFCl_2 : $m^* = 5.95 m_0$ and $m^* = 0.84 m_0$). This observation aligns well with results obtained for similar crystals CeX_3 (X=F, Cl, Br) [23, 24], $\text{CeCl}_{3-x}\text{Br}_x$ [7], and $\text{CeBr}_{3-x}\text{I}_x$ [8].

Chornodolskyy Ya.M. – Candidate of Physical and Mathematical Sciences, Associate Professor;
Karnaushenko V.O. – Doctor of Philosophy (Applied Physics and Nanomaterials), junior researcher;
Ihnatsevych S.O. – junior researcher;
Voloshinovskii A.S. – Doctor of Physical and Mathematical Sciences, Professor;
Syrotyuk S.V. – Candidate of Physical and Mathematical

Sciences, Associate Professor;
Vankevych P.I. – Doctor of Technical Sciences, Professor;
Bolkot P.A. – Doctor of Philosophy (Weapons and military equipment), senior researcher;
Derevjanchuk A.Y. – Candidate of Technical Sciences Professor.

- [1] C. Dujardin, E. Auffray, E. Bourret-Courchesne, et al. *Needs, trends, and advances in inorganic scintillators*, IEEE Transactions on Nuclear Science, 65(8), 1977 (2018); <https://doi.org/10.1109/TNS.2018.2840160>.
- [2] K. Shimamura, E. Villora, S. Nakakita, et al. *Growth and scintillation characteristics of CeF₃, PrF₃ and NdF₃ single crystals*, Journal of crystal growth, 264(1-3), 208 (2004); <https://doi.org/10.1016/j.jcrysgro.2003.12.018>.
- [3] F. Cappella, A. d'Angelo, and F. Montecchia, *Performances and potential of a CeCl₃ scintillator*, Nuclear Instruments and Methods in Physics Research Section A: Accelerators, Spectrometers, Detectors and Associated Equipment, 618(1-3), 168, (2010); <https://doi.org/10.1016/j.nima.2010.02.105>.
- [4] F. G. A. Quarati, P. Dorenbos, J. van der Biezen, et al. *Scintillation and detection characteristics of high-sensitivity CeBr₃ gamma-ray spectrometers*, Nuclear Instruments and Methods in Physics Research Section A: Accelerators, Spectrometers, Detectors and Associated Equipment, 729, 596 (2013); <https://doi.org/10.1016/j.nima.2013.08.005>.
- [5] A. Bessiere, P. Dorenbos, C.W.E. van Eijk, et al. *Luminescence and scintillation properties of the small band gap compound LaI₃: Ce³⁺*, Nuclear Instruments and Methods in Physics Research Section A: Accelerators, Spectrometers, Detectors and Associated Equipment 537(1-2), 22 (2005); <https://doi.org/10.1016/j.nima.2004.07.224>.
- [6] M. D. Birowosuto, P. Dorenbos, Novel γ - and X-ray scintillator research: on the emission wavelength, light yield and time response of Ce³⁺ doped halide scintillators, Physica status solidi (a), 206(1), 9 (2009); <https://doi.org/10.1002/pssa.200723669>.
- [7] Ya. M. Chornodolskyy, V. O. Karnaushenko, S. V. Syrotyuk, et al. *Energy structure of CeCl₂Br and CeClBr₂ crystals*, Journal of Physical Studies, 27(3), 3702 (2023); <https://doi.org/10.30970/jps.27.3702>.
- [8] K. Przystupa, Ya. M. Chornodolskyy, Ja. Selech, et al. *The Influence of Halide Ion Substitution on Energy Structure and Luminescence Efficiency in CeBr₂I and CeBrI₂ Crystals*, Materials, 16(14), 5085 (2023); <https://doi.org/10.3390/ma16145085>.
- [9] W. W. Moses, S. E. Derenzo, M. J. Weber, et al. *Scintillation mechanisms in cerium fluoride*, Journal of luminescence, 59(1-2), 89 (1994); [https://doi.org/10.1016/0022-2313\(94\)90026-4](https://doi.org/10.1016/0022-2313(94)90026-4).
- [10] K. Wei, Ch. Guo, J. Deng, Ch Shi, *Electronic structure of CeF₃ crystal*, Journal of electron spectroscopy and related phenomena, 79, 83 (1996); [https://doi.org/10.1016/0368-2048\(96\)02808-3](https://doi.org/10.1016/0368-2048(96)02808-3).
- [11] D. F. Anderson, *Cerium fluoride: a scintillator for high-rate applications*, Nuclear Instruments and Methods in Physics Research Section A: Accelerators, Spectrometers, Detectors and Associated Equipment, 287(3), 606 (1990); [https://doi.org/10.1016/0168-9002\(90\)91585-Y](https://doi.org/10.1016/0168-9002(90)91585-Y).
- [12] O. Guillot-Noël, J.T.M. de Haas, P. Dorenbos, et al. *Optical and scintillation properties of cerium-doped LaCl₃, LuBr₃ and LuCl₃*, Journal of luminescence 85(1-3), 21 (1999); [https://doi.org/10.1016/S0022-2313\(99\)00063-0](https://doi.org/10.1016/S0022-2313(99)00063-0).
- [13] E. V. D. van Loef, P. Dorenbos; C. W. E. van Eijk, et al. *High-energy-resolution scintillator: Ce³⁺ activated LaBr₃*, Applied physics letters, 79(10), 1573 (2001); <https://doi.org/10.1063/1.1385342>.
- [14] G. Ren, P. Yu, Ch. Xiaofeng, et al. *Growth, thermo-stability and radiation damage of cerium-doped lanthanum chloride (LaCl₃: Ce) scintillation crystal*, Nuclear Instruments and Methods in Physics Research Section A: Accelerators, Spectrometers, Detectors and Associated Equipment, 579(1), 11 (2007); <https://doi.org/10.1016/j.nima.2007.04.003>.
- [15] J. P. Perdew, *Density functional theory and the band gap problem*, International Journal of Quantum Chemistry 28(S19), 497 (1985); <https://doi.org/10.1002/qua.560280846>.
- [16] M. Nikl, *Wide band gap scintillation materials: progress in the technology and material understanding*, physica status solidi (a), 178(2), 595 (2000); [https://doi.org/10.1002/1521-396X\(200004\)178:2<595::AID-PSSA595>3.0.CO;2-X](https://doi.org/10.1002/1521-396X(200004)178:2<595::AID-PSSA595>3.0.CO;2-X).
- [17] M. Lewin, E. H. Lieb, and R. Seiringer, *The local density approximation in density functional theory*, Pure and Applied Analysis, 2(1), 35 (2020); <https://doi.org/10.2140/paa.2020.2.35>.
- [18] J. P. Perdew, K. Burke, and M. Ernzerhof, *Generalized gradient approximation made simple*, Physical review letters, 77(18), 3865 (1996); <https://doi.org/10.1103/PhysRevLett.77.3865>.
- [19] Data retrieved from the Materials Project for CeF₃ (mp-510560) from database version v2022.10.28. <https://doi.org/10.17188/1263001>.
- [20] Data retrieved from the Materials Project for CeCl₃ (mp-582011) from database version v2022.10.28. <https://doi.org/10.17188/1276931>.
- [21] Yu-Hong Dai, *A perfect example for the BFGS method*, Mathematical Programming, 138, 501 (2013); <https://doi.org/10.1007/s10107-012-0522-2>.

- [22] X. Gonze, B. Amadon, P.-M. Anglade, et al. *ABINIT: First-principles approach to material and nanosystem properties*, Computer Physics Communications, 180(12), 2582 (2009); <https://doi.org/10.1016/j.cpc.2009.07.007>.
- [23] Ya. M. Chornodolsky, V. O. Karнаushenko, V. V. Vistovsky, et al. *Energy band structure peculiarities and luminescent parameters of CeX₃ (X= Cl, Br, I) crystals*, Journal of Luminescence, 237, 118147 (2021); <https://doi.org/10.1016/j.jlumin.2021.118147>.
- [24] O. Kochan, Ya. Chornodolsky, Ja. Selech, et al. *Energy Structure and Luminescence of CeF₃ Crystals*, Materials 14(15), 4243 (2021); <https://doi.org/10.3390/ma14154243>.
- [25] M. Loyd, L. Stand, D. Rutstrom, et al. *Investigation of CeBr_{3-x}I_x scintillators*, Journal of Crystal Growth, 531, 125365 (2020); <https://doi.org/10.1016/j.jcrysgro.2019.125365>.
- [26] H. Wei, V. Martin, A. Lindsey, et al. *The scintillation properties of CeBr_{3-x}Cl_x single crystals*, Journal of luminescence 156, 175 (2014); <https://doi.org/10.1016/j.jlumin.2014.08.015>.

Я.М. Чорнодольський¹, В.О. Карнаушенко¹, С.О. Ігнацевич¹,
А.С. Волошиновський¹, С.В. Сиротюк², П.І. Ванкевич³, П.А. Болкот³,
А.Й. Дерев'янчук⁴

Енергетична структура змішаних галогенідних кристалів CeF₂Cl та CeFCl₂

¹Львівський національний університет імені Івана Франка, Львів, Україна, yaroslav.chornodolsky@lnu.edu.ua

²Національний університет "Львівська політехніка", Львів, Україна,

³Національна академія сухопутних військ імені гетьмана Петра Сагайдачного, Львів, Україна,

⁴Сумський державний університет, Суми, Україна

Розраховано зонні енергетичні структури кристалів CeF₂Cl та CeFCl₂ за допомогою методу проєкційних приєднаних хвиль (PAW) та гібридного обмінно-кореляційного функціоналу PBE0. Вершина валентної зони формується з 2р-станів F і 3р-станів Cl. В нижній частині зони провідності для обох кристалів між 5d-станами Ce спостерігається енергетична щілина, яка утворює дві підзони, 5d1 і 5d2, із різними ефективними масами електронів (2,49 m₀ і 0,19 m₀ для CeF₂Cl і 5,95 m₀ та 0,84 m₀ для CeFCl₂, відповідно). В забороненій зоні знаходяться 4f стани Ce. Отримані значення ширини забороненої зони кристалів CeF₂Cl та CeFCl₂ становлять 6 еВ та 4,6 еВ, відповідно.

Ключові слова: скінтілятор, зонна структура, густина станів, екситон, метод проєкційних приєднаних хвиль.